Article

Electrochemical Promotion of Nanostructured Palladium Catalyst for Complete Methane Oxidation

Yasmine M. Hajar, Balaji Venkatesh and Elena A. Baranova * [ID]

Department of Chemical and Biological Engineering, Centre for Catalysis Research and Innovation (CCRI), University of Ottawa, 161 Louis-Pasteur, Ottawa, ON K1N 6N5, Canada; yhaja059@uottawa.ca (Y.M.H.); bvenk044@uottawa.ca (B.V.)

* Correspondence: elena.baranova@uottawa.ca; Tel.: +1-6135625800 (ext. 6302); Fax: +1-6135625172

check for updates

Abstract: Electrochemical promotion of catalysis (EPOC) was investigated for methane complete oxidation over palladium nano-structured catalysts deposited on yttria-stabilized zirconia (YSZ) solid electrolyte. The catalytic rate was evaluated at different temperatures (400, 425 and 450 °C), reactant ratios and polarization values. The electrophobic behavior of the catalyst, i.e., reaction rate increase upon anodic polarization was observed for all temperatures and gas compositions with an apparent Faradaic efficiency as high as 3000 (a current application as low as 1 μA) and maximum rate enhancement ratio up to 2.7. Temperature increase resulted in higher enhancement ratios under closed-circuit conditions. Electrochemical promotion experiments showed persistent behavior, where the catalyst remained in the promoted state upon current or potential interruption for a long period of time. An increase in the polarization time resulted in a longer-lasting persistent promotion (p-EPOC) and required more time for the reaction rate to reach its initial open-circuit value. This was attributed to continuous promotion by the stored oxygen in palladium oxide, which was formed during the anodic polarization in agreement with p-EPOC mechanism reported earlier.

Keywords: electrochemical promotion; NEMCA; palladium; ionic promoter; nanoparticles; yttria-stabilized zirconia

1. Introduction

Natural Gas Vehicles (NGVs) have gained considerable attention in the last decade due to much lower greenhouse gas emissions and lower price of methane compared to diesel or gasoline. Not only CH_4 is abundant in natural gas form, but methane can also be produced using anaerobic digestion technologies of bio-derived sources [1–4]. Despite lower emissions of NGVs they often suffer from incomplete methane combustion. Because methane is also 23 times more potent in warming the atmosphere than carbon dioxide its complete conversion to CO_2 is paramount. Therefore, the development of efficient low temperature catalysts for deep oxidation of methane (CH_4) has recently attracted significant attention [5–10].

Palladium-based catalysts are considered the most efficient for methane activation in excess of oxygen and their activity depends on temperature, methane/oxygen ratio, and catalyst surface oxidation state and composition [5]. The nature of the active surface sites PdO_x vs. Pd was a subject of several studies [6,7]. It was shown that chemisorbed oxygen on Pd metal is poorly active, whereas Pd oxidation with an optimum of 3–4 monolayers forms an active PdO catalyst. Chemisorption of a first layer of oxygen is fast; however, partial bulk oxidation is relatively slow [7].

The innovative field of catalysis that could boost complete methane oxidation reaction over Pd is electrochemical promotion of catalysis (EPOC) or non-Faradaic electrochemical modification of catalytic activity (NEMCA). This general, well-established phenomenon in catalysis aims at controlling

in-situ both the activity and the selectivity of a catalyst through application of electric stimuli [8–11]. EPOC is observed with solid electrolyte materials that serve as catalyst support. Ions contained in these electrolytes (O^{2-}, H^+, Na^+ OH^-, etc.) are electrochemically pumped to the catalyst surface, where they act as promoting species leading to modification of catalyst electronic properties and as a result its catalytic activity and selectivity. More precisely, applying an anodic polarization results in the strengthening of electron-donor adsorbates, e.g., chemisorbed methane, and weakening of the binding strength of electron-accepting adsorbates, e.g., dissociatively chemisorbed oxygen [12]. The resulting electrochemical activation magnitude is much higher than that predicted by Faraday's law. [13,14]. The increase in the catalytic rate, Δr (mol O/s) divided by the electrochemical rate, I/nF (I is current, F is Faraday's constant and n is number of electrons, 2 for O^{2-}) is denoted as the apparent Faradaic efficiency, Λ, and the process is considered non-Faradaic when $|\Lambda|$ is greater than 1. Another parameter used to quantify EPOC is the rate enhancement ratio, ρ, which is the ratio between the promoted closed-circuit catalytic rate, r and the unpromoted open-circuit catalytic rate, r_o.

　　　The electrochemical promotion of complete methane oxidation was investigated on palladium catalysts prepared using various methods as summarized in Table 1 [15–23]. Electrochemical promotion of Pd thick film catalyst electrode prepared using wet impregnation was investigated in the temperature range of 470–600 °C [18]. The rate enhancement of 40% and an apparent Faradaic efficiency of 1.85 were found in this work. The addition of CeO_2 layer between the YSZ solid-electrolyte and Pd film catalyst increased the open-circuit catalytic rate but decreased the apparent Faradaic efficiency due to the higher electric resistance [18]. Another study on a Pd film catalyst prepared using commercial organometallic paste showed higher enhancement ratio (ρ = 5.6) and Faradaic efficiency (Λ = 579) at 560 °C; however, instability of the catalyst over time and rapid deactivation within 900 min of experiment was also noted [20]. Furthermore, the effect of CeO_2 layer was studied in [24]. It was shown that presence of ceria increased catalytic activity of Pd due to the formation of an active PdO phase, which was stabilized by CeO_2 acting as a continuous source of oxygen, similarly to the oxygen migration from the YSZ electrolyte under EPOC. In another study, an addition of porous YSZ layer between Pd film-catalyst and the dense YSZ solid-electrolyte resulted in a high open-circuit catalytic rate. The authors reported an enhancement ratio of 1.2 and apparent Faradaic efficiency, Λ, of 17 under fuel-rich conditions [23]. EPOC of sputtered Pd catalyst-electrode was compared to impregnated Pd for methane complete oxidation. The sputtered catalysts showed slightly higher Λ of 12 but similar enhancement ratio (ρ = 1.6) [21]. The effect of metal loading and catalyst thickness on EPOC of Pd was studies on Pd catalyst prepared by physical vapor deposition (PVD). It was found that metal loading and catalyst thickness have significant effect on the open-circuit rate and electrochemical promotion, where the thinner films resulted in the highest reaction rates per gram of catalyst at 500 °C [17]. A scaling-up of the system was attempted by electroless deposition of Pd in the channels of a YSZ monolith honeycomb; however, decrease in the conversion of methane occurred under positive and negative polarization [19].

　　　Therefore, from previous EPOC studies on Pd for complete CH_4 oxidation, it is clear that the catalyst preparation method has a strong influence on Pd morphology, structure, oxidation state and as a result, on its catalytic activity, degree of promotion and stability under open and closed circuit conditions. Furthermore, from the practical point of view it is essential to work with low loadings of noble-metal catalysts that exhibit high dispersion and large active surface area In the present work, we report electrochemical promotion of nano-structured, highly dispersed Pd catalyst prepared by polyol reduction method for CH_4 complete oxidation in the temperature range of 400 and 450 °C and various gas compositions.

Table 1. Summary of EPOC tests performed for methane oxidation on Pd-YSZ support.

Catalyst Synthesis Method	Loading	I or U Applied	T/°C	P_{CH4}/kPa	P_{O2}/kPa	Total Flow/ccm	Rate Change/mol O.s^{-1} 10^{-8}	ρ	Λ	Authors, Year & Ref.
Paste coating	n/a	+300 μA	400	2.75	1.55	n/a	4.52 to 20.5	4.5	103	[a] Giannikos et al. (1998) [15]
Paste coating	n/a	+1 V	400	2.6	1.9	n/a	0.295 to 20	68	153	[a] Frantzis et al. (2000) [16]
PVD	24 μg	+100 μA	500	2	10	166	7.3 to 20.4	2.8	258	Roche et al. (2008) [17]
Thermal decomposition	1.1 mg/cm^2	+10 mA	600	0.4	1	150	0.47 to 0.68	2.6	<1	[a,b] Jimenez-Borja et al. (2009) [18]
Electroless deposition	5 mg total	+100 μA	400	2	10	166	136.4 to 135.2	0.99	−23	Roche et al. (2010) [19]
Paste coating	7 mg/cm^2	+25 μA	560	0.4	1.2	150	1.6 to 9.1	5.6	579	[a] Jimenez-Borja et al. (2011) [20]
Sputtered	0.4 mg/cm^2	+1 mA	350	1.3	4.5	200	11.4 to 18.2	1.6	12	Matei et al. (2012) [21]
Impregnation	0.4 mg/cm^2	+300 μA	350	1.3	4.5	200	22 to 26	1.18	25	Jimenez-Borja et al. (2012) [22]
Impregnation	0.4 mg/cm^2	+5 mA	400	1.4	2.8	200	135 to 158	1.2	17	Matei et al. (2013) [23]
Polyol method	0.3 mg/cm^2	+0.5 V	425	2	4	100	6 to 16	2.66	383	[a] This work

[a] Continuous increase in closed-circuit rate post EPOC; [b] Electrolysis effect.

2. Results and Discussion

Transmission electron microscopy (TEM) was used to determine the palladium morphology and particle size (Figure 1a,b). The resulting Pd particles are spherical in shape with a diameter of approximately 5 nm, that are coalesced together in larger aggregates of roughly 50 nm in size. Figure 1c,d shows SEM images of as-prepared Pd/YSZ catalysts and the same catalyst after catalytic measurements under open circuit and EPOC conditions. It can be seen that as-prepared catalyst-electrode forms a highly dispersed, non-continuous layer on YSZ surface that consists of fine grains and pores. After the reaction, the "spent" catalyst shows much larger catalyst islands indicating a change in the morphology due to the catalyst agglomeration that takes place during the reaction. The resulting energy dispersive X-ray spectroscopy (EDS) spectrum (Figure 2a) of as-prepared Pd shows that the only element present is Pd. The x-ray diffraction pattern (XRD) contains several diffraction peaks of Pd (111), (200) and (220) corresponding to face-centered cubic (fcc) structure typical for bulk palladium metal. The crystallite size of Pd found from Pd (111) was 8 nm.
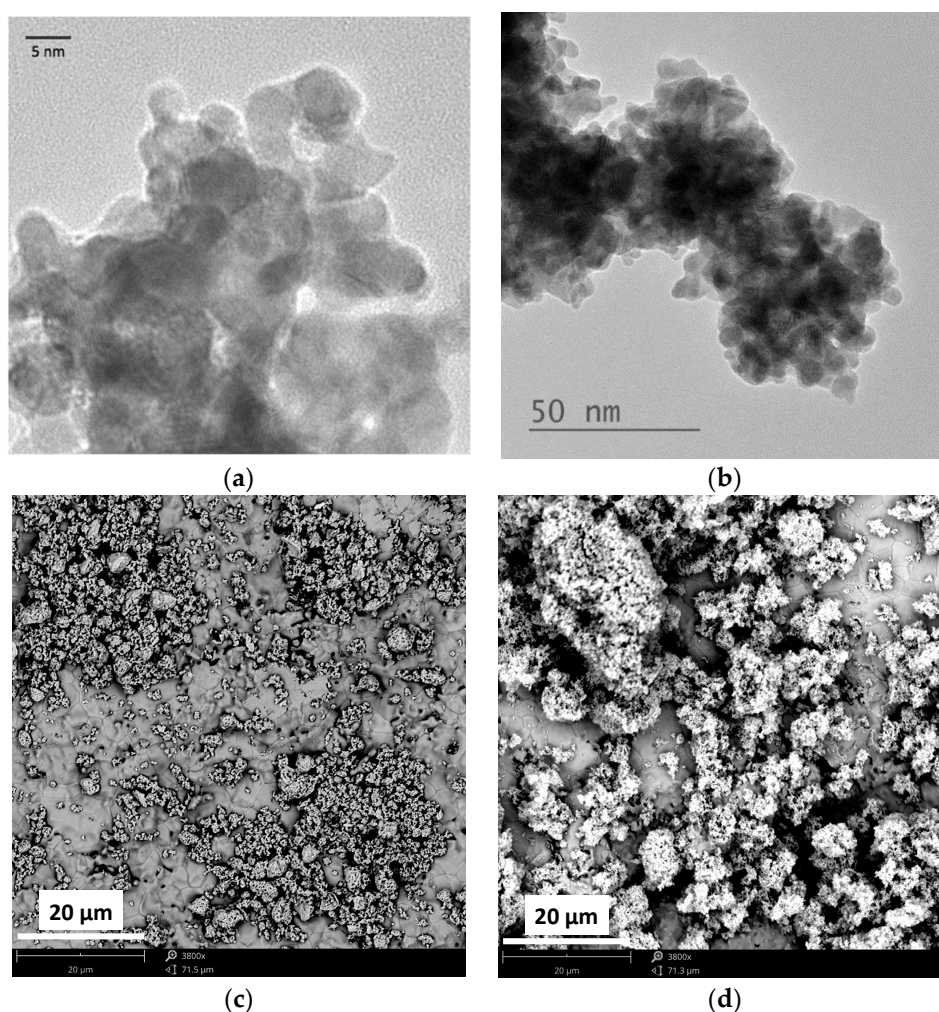

Figure 1. (**a**,**b**) TEM images of stand-alone Pd NPs at 5 nm and 50 nm scale; (**c**,**d**) SEM images of as-prepared (**c**) and post-experiment (**d**) Pd catalyst deposited on YSZ solid electrolyte.
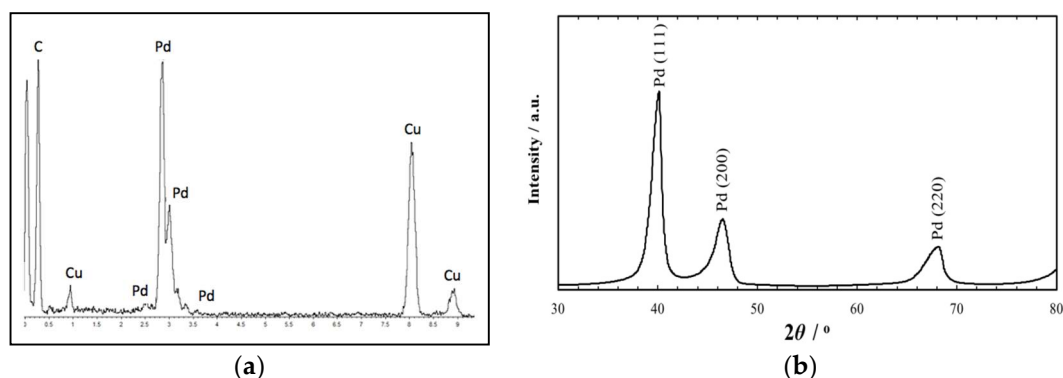
Figure 2. (**a**) EDS spectrum and (**b**) XRD pattern of Pd catalyst.

The open-circuit catalytic rate of methane oxidation was tested at two different temperatures and at various gas compositions (Figure 3). It can be seen that for both temperatures the rate increased as a function of oxygen partial pressure. The increase was more significant at 4 kPa of methane where oxygen-to-methane partial pressures ratios were lower. The rate increase in fuel-rich condition is indicative of a Langmuir-Hinshelwood mechanism [15] where methane is able to competitively adsorb on palladium as seen at 450 °C under 4 kPa of CH_4, while the quasi-stable value at higher ratio of oxygen (at 2 kPa of CH_4) can be explained by an Eley-Rideal mechanism as CH_4 reacts on the oxygen covered surface [25].
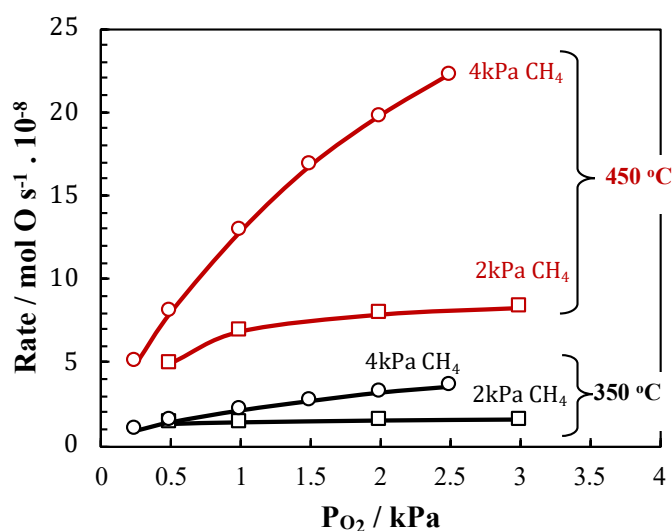

Figure 3. Effect of oxygen-to-methane ratio on catalytic rate at 350 and 450 °C.

Figure 4 shows the transient rate response to an application of positive current (20 μA) between the Pd working electrode and the counter electrode at 450 °C. Under open-circuit conditions (t < 0.5 h), the catalytic rate was at 8.35×10^{-8} mol/s. When a constant current was imposed, the reaction rate gradually increased due to pumping of O^{2-} promoters to the catalyst surface. After 2 h of polarization, the closed-circuit rate increase was 180% higher than its corresponding open-circuit value. In addition, the non-Faradaic behavior resulted in an apparent Faradaic efficiency, Λ, of 610 denoting that the back-spillover of O^{2-} at a I/2F rate gave a 610 times increase in the overall oxidation rate [26]. It should be noted that slight increase in the catalyst-working electrode potential (U_{WR}) was observed upon positive polarization (from 0.39 to 0.42 V). Furthermore, the slow reaction rate increase did not reach a steady-state value even after 2 h of applied polarization and took over 1 h to reach the open circuit value observed before polarization. According to the mechanism of EPOC the reaction rate is due to the supply of oxygen ionic species from YSZ and the formation of an effective double

layer at the surface of the catalyst that changes the work function of Pd leading to weakening of the chemisorbed oxygen bond strength thus facilitating the –O_2C desorption from the catalyst surface.

A similar behavior was observed under potentiostatic conditions (U_{WR} = 0.25 V) and a stoichiometric flow of reactants at 425 °C (Figure 5). The catalytic rate slowly increased in value until it reached 7.0×10^{-8} mol s^{-1} after 2 h. As in the galvanostatic conditions (Figure 4) the closed-circuit reaction rate was continuously increasing with time without reaching a steady-state. After 2 h, the rate enhancement ratio of 1.31 and, an apparent Faradaic efficiency of 1107 were obtained. The high Λ value is due to the low current that passed through the cell, which was sufficient to promote Pd catalyst.
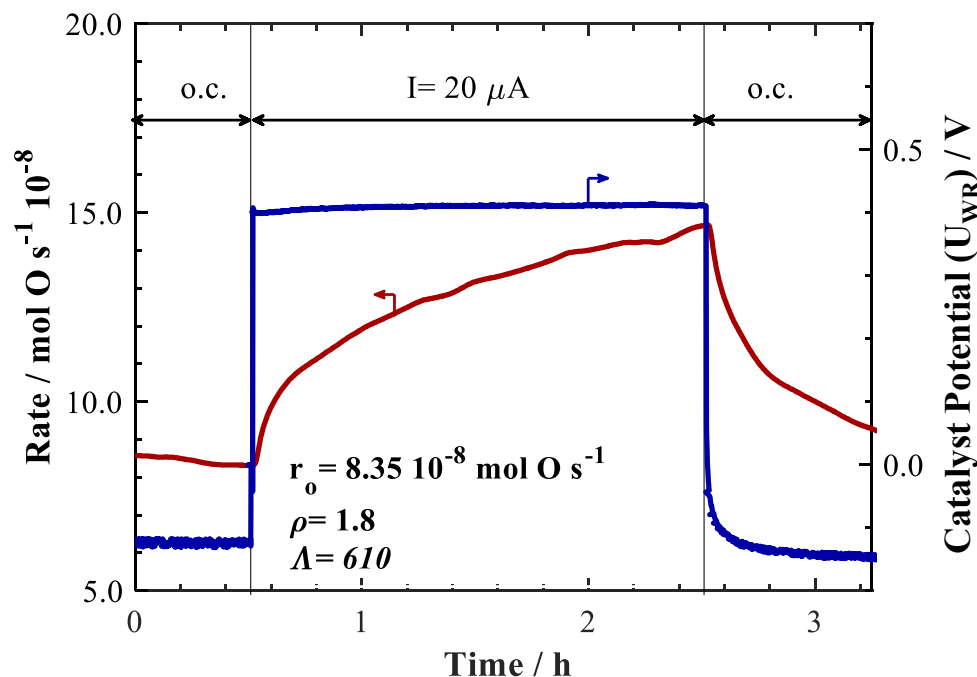

Figure 4. Transient rate response of Pd nanoparticles to a current step change. o.c.: open-circuit. Conditions: T = 450 °C, 2 kPa of CH_4 and 4 kPa of O_2. Flow rate: 100 ccm.

The continuous increase of the catalytic rate in Figures 4 and 5 can be explained by the continuous oxidation of palladium catalyst to PdO_x, which makes the catalyst more active for methane oxidation. In Figure 5, this continuous increase in catalytic rate occurred simultaneously with a decrease in current at a constant applied potential value indicating Pd oxide formation. Upon current or potential interruption the rate slowly returned to its initial state, because oxygen species stored in PdO_x continued acting as sacrificial promoters for methane oxidation reaction.
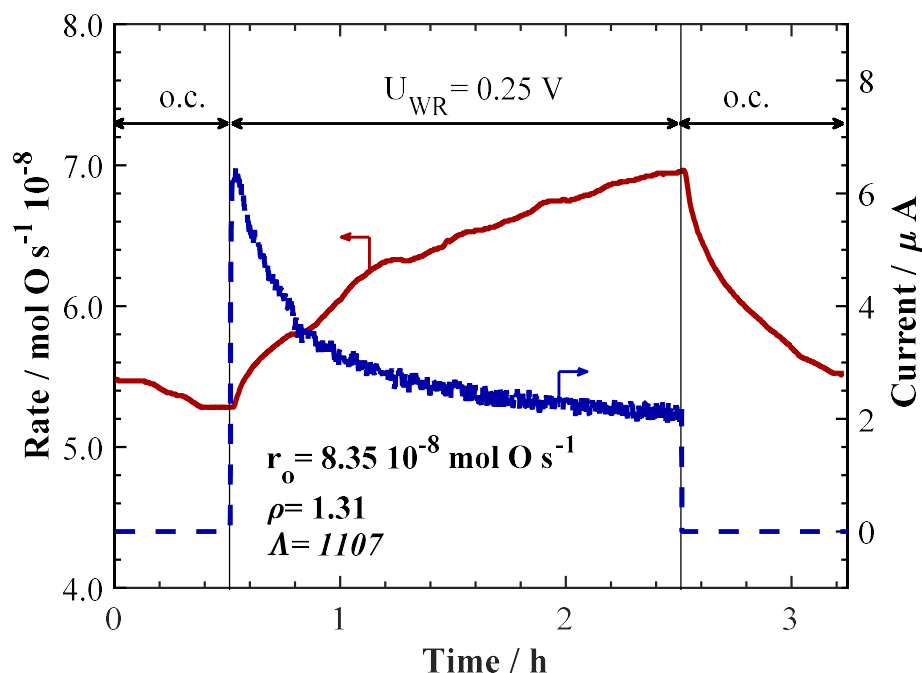
Figure 5. Transient rate response of Pd nanoparticles to potential step changes. o.c.: open-circuit. Conditions: T = 425 °C, 2 kPa of CH_4 and 4 kPa of O_2. Flow rate: 100 ccm.

To confirm PdO_x formation and oxygen storage effect on p-EPOC, the catalyst was polarized for a different duration 3, 6 and 10 h. As seen in Figure 6, the closed-circuit catalytic rate was continuously increasing with time under constant current (40 µA for 3 h) and potential (0.5 V for 6 and 10 h) application. It can be seen that even after ten hours of polarization, the closed-circuit rate kept on rising without reaching a steady-state. At the same time, the longer polarization time resulted in longer decrease of the open-circuit rate after polarization was stopped. A proportional relationship (as shown in the inset Figure 6) was found between the duration of EPOC and the time to reach the open-circuit rate $r_{o.c.}$. The slope of this relationship was 0.5. This persistent electrochemical promotion (p-EPOC) is due to the stored oxygen ions in PdO_x that act as sacrificial promoters when the electrical circuit is open [27].
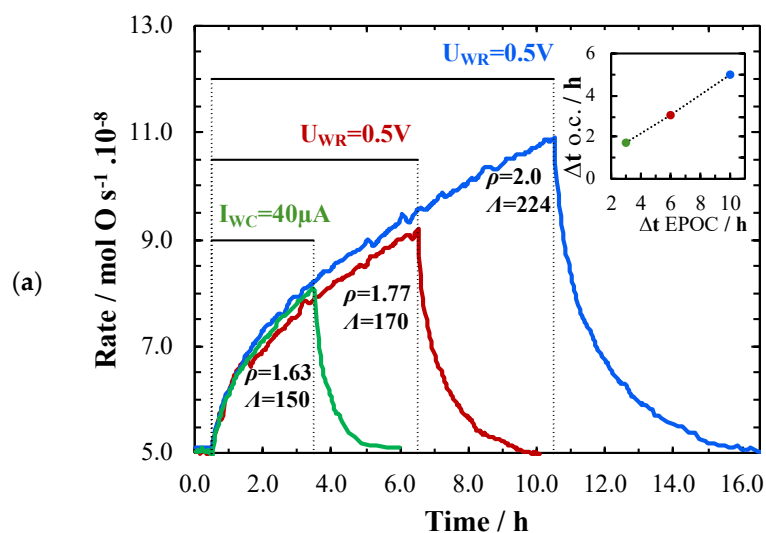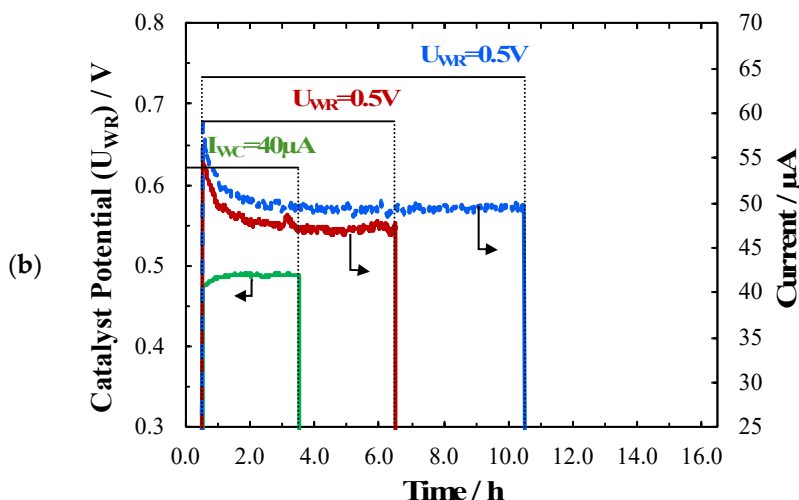

Figure 6. *Cont.*

Figure 6. (**a**) Transient rate response of Pd at different duration of EPOC and (**b**) the potential/current read at potentiostatic or galvanostatic application. Conditions: T = 425 °C, 2 kPa of CH_4 and 4 kPa of O_2. Flow rate: 100 ccm.

This indicates that during the positive polarization two parallel processes take place: i. Migration of $O^{\delta-}$ promoters to the gas exposed catalyst surface and ii PdO_x formation at the three-phase boundary (tpb) according to the electrochemical reaction:

$$Pd + xO^{2-} \rightarrow PdO_x + xe^- \quad (1)$$

Current decrease and potential increase upon positive potentiostatic (Figures 5 and 6) and glavanostatic polarization (Figure 4), respectively, confirms the formation of PdO_x. Palladium oxide has lower conductivity than Pd metal, therefore current that flows through the solid-state cell or potential difference of the working catalyst-electrode (U_{WR}) are the clear indication of an electrochemical oxide formation [28].

Figure 7 shows a transient rate response at a constant applied potential 0.5 V for 24 h. The reaction rate continuously increased for up to 20 h followed by 2 h of a steady-state rate and then a slight rate decrease. The continuous rate increase indicates constant catalyst activation due to the growth of PdO_x, whereas somewhat rate decrease after 22 h of polarization at 425 °C may be linked with morphology change observed for the "spent" catalysts (Figure 1d). The open-circuit rate took more than 6 h to return to its initial value showing a persistent promotional effect.
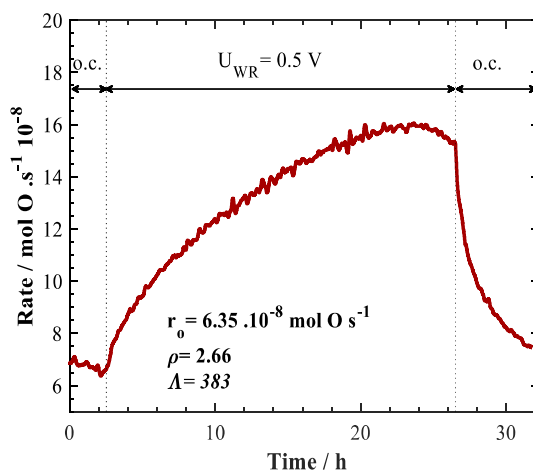

Figure 7. Long period transient rate response of Pd to a potentiostatic step change. o.c.: open-circuit. Conditions: T = 425 °C, 2 kPa of CH_4 and 4 kPa of O_2. Flow rate: 100 ccm.

Figure 8 shows the catalytic rate and catalyst potential change upon application of constant current as low as 1 μA. This resulted in the continuous catalytic rate increase for 1, 2 and 4 kPa of O_2, accompanied by catalyst potential (U_{WR}) increase, confirming palladium oxide formation. The corresponding Λ values are summarized in Figure 9.
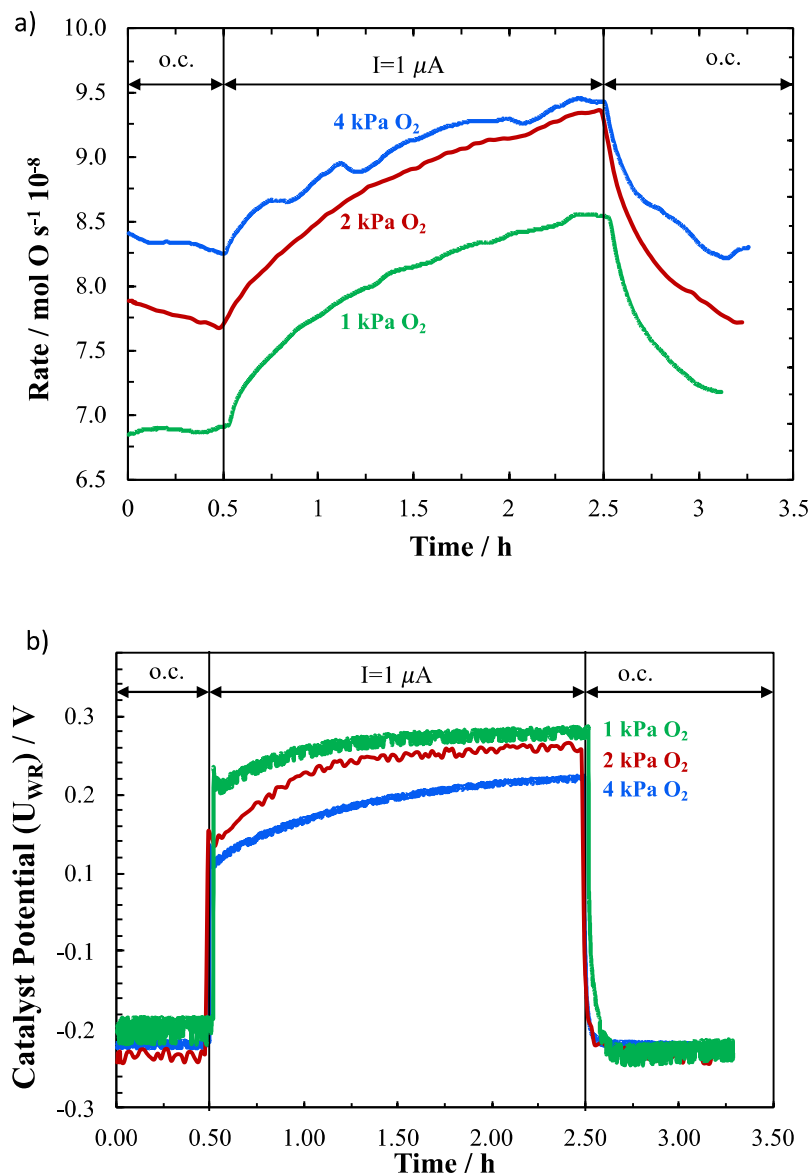

Figure 8. (**a**)Transient rate response of Pd catalyst at different O_2 partial pressure under 1 μA galvanostatic application and (**b**) the corresponding catalyst potential response. Conditions: T = 450 °C, 2 kPa of CH_4. Flow rate: 100 ccm.

In Figure 9, the effect of partial pressure on closed-circuit reaction rate was tested at different galvanostatic conditions. The highest increase in catalytic rate was found at slightly fuel-rich conditions resulting in a ρ value of 1.3; the higher rate can be explained by the advantaged adsorption of gaseous methane over oxygen. At this condition, gaseous methane can be expected to directly adsorb onto Pd, resulting in a competition between oxygen and methane adsorption following a Langmuir-Hinshelwood mechanism. In addition, the desorption of oxygen from the surface becomes facilitated at lower oxygen partial pressure in the atmosphere as the overall chemical potential of oxygen is reduced [29]. At a partial pressure ratio higher than the stoichiometric ratio, it is perceived that the catalytic rate increase is slightly lower. The slight decrease in the enhancement is due to the

competing adsorption of oxygen on the surface of Pd, putting slight mass-transfer limitations on the chemisorption of CH_4.
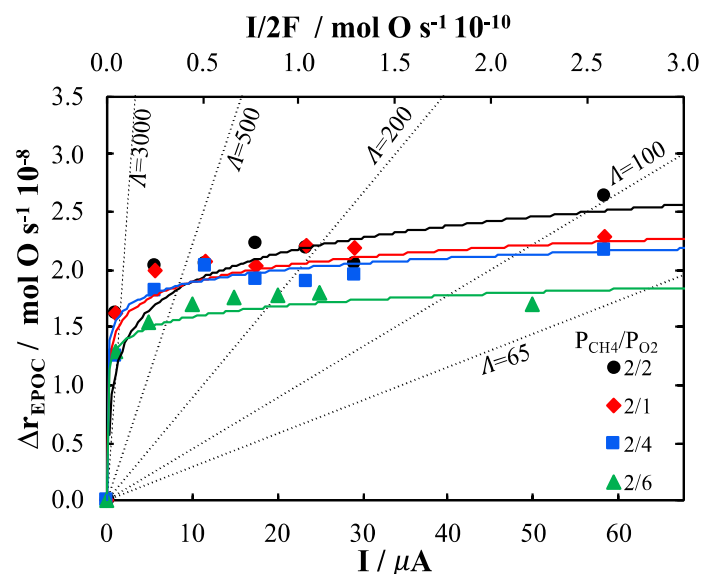

Figure 9. Current effect on catalytic rate in function of methane/oxygen ratio. T = 450 °C. Flow rate: 100 ccm.

Similarly, the effect of temperature on closed-circuit reaction rate was tested at different galvanostatic conditions. Figure 10 shows that there is an increase in catalytic rate as a function of temperature at all applied positive current values for 400, 425 and 450 °C. It can be noticed that upon application of small current of 1 μA, a significant rate increase was detected, resulting in a logarithmic-shape relationship of rate increase versus applied current. In addition, a highest value of ~2400 was found for the apparent Faradaic efficiency, constructing that a very minimal current was able to result in a change of the Pd surface oxidation state and hence the adsorption strength of methane reactant [15,16,18,20].
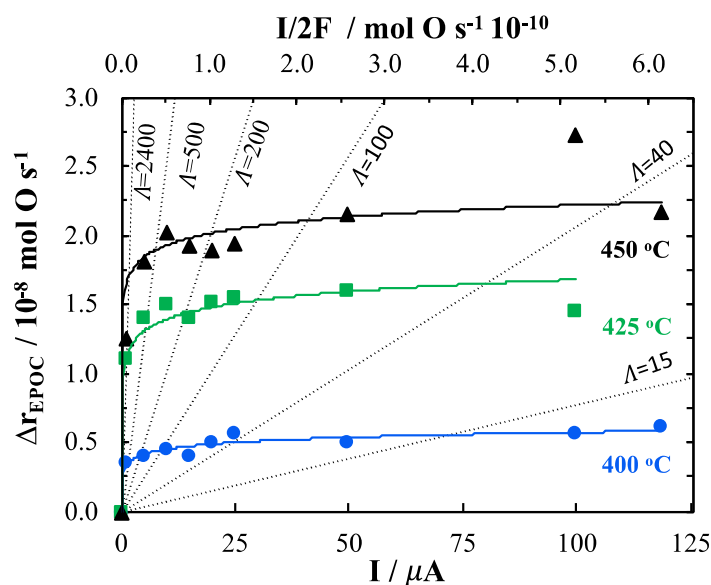

Figure 10. Current effect on catalytic rate in function of temperature: 400, 425 and 450 °C. P_{CH4} = 2 kPa and P_{O2} = 4 kPa. Flow rate: 100 ccm.

Table 1 compares EPOC of methane oxidation on Pd/YSZ found in this work to previous studies carried out on Pd catalyst-electrode deposited on YSZ solid-electrolyte. The table depicts where our results fall in comparison with previous experiments. It should be noted that the metal loading used in this work is the lowest in the temperature range of interest (T ≤ 450 °C), which is important for cold-start emission application. In agreement with previous work, Pd nanostructured catalyst synthesized by polyol method shows electrophobic type of EPOC, where only positive polarization promotes the reaction. Applied polarization led to the supply of $O^{\delta-}$ promoters from YSZ electrolyte to the catalyst surface, resulting in the formation of a more active phase of PdO, on the surface first and in the bulk gradually.

Ionic oxygen migration to the surface altered the adsorption properties of the catalyst surface, resulting in the weakening of gaseous oxygen adsorption and strengthening that of electron-donor methane. The alteration of the catalytic oxidation state was similar under both potentiostatic and galvanostatic application, which have resulted in a continuous increase in catalytic rate and a very slow open circuit rate decrease when the circuit was interrupted. This was explained by the formation of PdO during polarization and oxygen storage in its bulk, which was continuously providing the promoting oxygen species to the surface post-polarization according to p-EPOC mechanism [27].

3. Experimental

3.1. Synthesis of Pd Nanoparticles

Mono-metallic Pd NPs were synthesized using 0.133 g of palladium chloride (Fisher Scientific®, Canada) precursor salts dissolved in 25 mL of ethylene glycol and 0.8 M NaOH. The mixture was heated up to 160 °C and kept under stirring conditions for 3 h. The final colloidal solution was cooled down and washed repeatedly with ethanol.

3.2. Catalyst Characterization

X-ray diffraction (XRD) was performed on the fresh Pd sample using Rigaku Ultima IV multipurpose diffractometer (Rigaku, The Woodlands, TX, USA). The diffractometer was equipped with an X'Celerator detector with monochromatic CuKα radiation (λ = 1.5418 Å) at 40 kV and 44 mA with a divergence slit of 2/3 degree, a scan speed of 0.03 °/s and a scan step of 0.02 degrees between 30 and 80° 2θ.

The transmission electron microscopy (TEM) micrographs were obtained using JEOL JEM 2100F FETEM (JEOL, Peabody, MA, USA) operating with a field emission gun at an acceleration voltage of 200 kV. SEM micrographs were recorded using Phenom™ SEM (Nanoscience Instruments, Virginia, USA). Additional elemental analysis was performed using the energy dispersive X-ray spectroscopy (EDS) attachment.

3.3. Electrochemical Cell and Reactor

The solid electrolyte is a 19 mm diameter and 1 mm thickness disk of 8 mol % Y_2O_3-stabilized ZrO_2 (YSZ) (TOSOH®, Grove city, OH, USA) fabricated following the procedure reported earlier [30]. Inert gold reference and counter electrodes were deposited on one side of the disk by applying thin gold paste coating (Gwent Group, Pontypool, UK) of 0.2 and 1 cm^2 surface areas, respectively. This was followed by annealing in air at 500 °C. The catalyst-working electrode was deposited on the other side of the solid electrolyte disk (1 cm^2 surface area) opposing to the counter electrode. To this end, mono-metallic Pd were dispersed in isopropanol and 10 μL of a suspension were deposited at a time with intermediate drying at room temperature. The resulting total metal loading was 0.5 mg of Pd on YSZ. Catalytic measurements were carried out at atmospheric pressure in the single-chamber capsule reactor reported earlier [31,32]. The working electrode side of the electrolyte was pressed against a gold mesh (1 cm^2) that served as a current collector, while the counter and reference electrodes were

pressed directly against gold wires [33]. Two type K thermocouples (Omega®, Quebec, Canada) were placed in vicinity of the electrochemical cell, one for temperature control and one for data acquisition.

3.4. Catalytic and Electrochemical Measurements

The reaction gases were CH_4 (Linde, 99.99%), O_2 (Linde, 99.99%), and He (Linde, 99.997%) as a carrier gas. The total flow rate was constant at 100 mL min^{-1}. Gas composition was varied using MKS, 1259 C and 1261-C series flow meters and detected using non-dispersive infrared (NDIR) CO_2 gas analyzer (Horiba, VA-3000, Burlington, Canada). Constant electric current or potential were applied using a potentiostat-galvanostat (Arbin Instruments®, MSTAT, College Station, TX, USA) connected to the electrodes of solid-electrolyte electrochemical cell.

4. Conclusions

Electrochemical promotion of Pd nanostructured catalyst was investigated for the methane oxidation reaction in the 400–450 °C temperature range. The promotion of the catalytic rate of Pd NPs was achieved under anodic polarization. Upon various potentiostatic and galvanostatic tests, non-Faradaic enhancement was achieved, most notably at 450 °C, under the application of 1 μA, where Λ was equal to ~3000, higher than any previous EPOC study on Pd. Continuous increase in the reaction rate was found under EPOC conditions, due to the Pd oxide formation in the vicinity of the tpb. A proportional relationship was found between the duration of polarization and the post-polarization time required to reach the initial open-circuit rate value. Post polarization, a persistent promotion (p-EPOC) was observed due to the promotion of the reaction by the stored oxygen, which was accumulated during positive polarization. Overall, our work revealed interesting behavior of Pd synthesized by polyol method, providing further insight into the application of electrochemical promotion for complete methane oxidation with highly dispersed Pd.

Author Contributions: Conceptualization, E.A.B.; Data curation, Y.M.H and B.V.; Formal analysis, B.V.; Funding acquisition, E.A.B.; Methodology, Y.M.H.; Project administration, E.A.B.; Supervision, E.A.B.; Validation, Y.M.H.; Writing—original draft, Y.M.H.; Writing—review & editing, E.A.B.

Conflicts of Interest: The authors declare no conflict of interest.

References

1. Demirbaş, A. Biomass resource facilities and biomass conversion processing for fuels and chemicals. *Energy Convers. Manag.* **2001**, *42*, 1357–1378. [CrossRef]
2. Cheng, H.; Hu, Y. Municipal solid waste (MSW) as a renewable source of energy: Current and future practices in China. *Bioresour. Technol.* **2010**, *101*, 3816–3824. [CrossRef] [PubMed]
3. Tripathi, M.; Sahu, J.N.; Ganesan, P. Effect of process parameters on production of biochar from biomass waste through pyrolysis: A review. *Renew. Sustain. Energy Rev.* **2016**, *55*, 467–481. [CrossRef]
4. Xiao, Y.; He, P.; Cheng, W.; Liu, J.; Shan, W.; Song, H. Converting solid wastes into liquid fuel using a novel methanolysis process. *Waste Manag.* **2016**, *49*, 304–310. [CrossRef] [PubMed]
5. Farrauto, R.J.; Hobson, M.C.; Kennelly, T.; Waterman, E.M. Catalytic chemistry of supported palladium for combustion of methane. *Appl. Catal. A Gen.* **1992**, *81*, 227–237. [CrossRef]
6. Ciuparu, D.; Lyubovsky, M.R.; Altman, E.; Pfefferle, L.D.; Datye, A. Catalytic combustion of methane over palladium-based catalysts. *Catal. Rev. Sci. Eng.* **2002**, *44*, 593–649. [CrossRef]
7. Burch, R.; Urbano, F.J. Investigation of the active state of supported palladium catalysts in the combustion of methane. *Appl. Catal. A Gen.* **1995**, *124*, 121–138. [CrossRef]
8. Boudart, M.; Djega-Mariadassou, G. *Kinetics of Heterogeneous Catalytic Reactions*; Princeton University Press: Princeton, NJ, USA, 1984.
9. Campbell, I.M. *Catalysis at Surfaces*; Springer Science & Business Media: New York, NY, USA, 1988.

10. Vayenas, C.G.; Bebelis, S.; Neophytides, S. Non-Faradaic Electrochemical Modification of Catalytic Activity. *J. Phys. Chem.* **1988**, *92*, 5083–5085. [CrossRef]

11. Ladas, S.; Kennou, S.; Bebelis, S.; Vayenas, C.G. Origin of non-faradaic electrochemical modification of catalytic activity. *J. Phys. Chem.* **1993**, *97*, 8845–8848. [CrossRef]

12. Nicole, J.; Tsiplakides, D.; Pliangos, C.; Verykios, X.E.E.; Comninellis, C.; Vayenas, C.G.G. Electrochemical Promotion and Metal–Support Interactions. *J. Catal.* **2001**, *204*, 23–34. [CrossRef]

13. Vayenas, C.G.; Bebelis, S.; Ladas, S. Dependence of catalytic rates on catalyst work function. *Nature* **1990**, *343*, 625–627. [CrossRef]

14. Vayenas, C.G.; Bebelis, S.; Pliangos, C.; Brosda, S.; Tsiplakides, D. *Electrochemical Activation of Catalysis: Promotion, Electrochemical Promotion, and Metal-Support Interactions*; Springer: New York, NY, USA, 2001. [CrossRef]

15. Giannikos, A.; Frantzis, A.D.; Pliangos, C.; Bebelis, S.; Vayenas, C.G. Electrochemical promotion of CH_4 oxidation on Pd. *Ionics (Kiel)* **1998**, *4*, 53–60. [CrossRef]

16. Frantzis, A.D.; Bebelis, S.; Vayenas, C.G. Electrochemical promotion (NEMCA) of CH_4 and C_2H_4 oxidation on Pd/YSZ and investigation of the origin of NEMCA via AC impedance spectroscopy. *Solid State Ionics* **2000**, *136–137*, 863–872. [CrossRef]

17. Roche, V.; Karoum, R.; Billard, A.; Revel, R.; Vernoux, P. Electrochemical promotion of deep oxidation of methane on Pd/YSZ. *J. Appl. Electrochem.* **2008**, *38*, 1111–1119. [CrossRef]

18. Jiménez-Borja, C.; Dorado, F.; de Lucas-Consuegra, A.; García-Vargas, J.M.; Valverde, J.L.J.L. Complete oxidation of methane on Pd/YSZ and Pd/CeO_2/YSZ by electrochemical promotion. *Catal. Today* **2009**, *146*, 326–329. [CrossRef]

19. Roche, V.; Revel, R.; Vernoux, P. Electrochemical promotion of YSZ monolith honeycomb for deep oxidation of methane. *Catal. Commun.* **2010**, *11*, 1076–1080. [CrossRef]

20. Jiménez-Borja, C.; Dorado, F.; Consuegra, A.D.; Vargas, J.M.G.; Valverde, J.L. Electrochemical Promotion of CH_4 Combustion over a Pd/CeO_2-YSZ Catalyst. *Fuel Cells* **2011**, *11*, 131–139. [CrossRef]

21. Matei, F.; Ciuparu, D.; Jiménez-Borja, C.; Dorado, F.; Valverde, J.L.; Brosda, S. Electrochemical promotion of methane oxidation on impregnated and sputtered Pd catalyst-electrodes deposited on YSZ. *Appl. Catal. B Environ.* **2012**, *127*, 18–27. [CrossRef]

22. Jimenez-Borja, C.; Brosda, S.; Matei, F.; Makri, M.; Delgado, B.; Sapountzi, F.; Ciuparu, D.; Dorado, F.; Valverde, J.L.; Vayenas, C.G. Electrochemical promotion of methane oxidation on Pd catalyst-electrodes deposited on Y_2O_3-stabilized-ZrO_2. *Appl. Catal. B Environ.* **2012**, *128*, 48–54. [CrossRef]

23. Matei, F.; Jimenez-Borja, C.; Canales-Vazquez, J.; Brosda, S.; Dorado, F.; Valverde, J.L.; Ciuparu, D. Enhanced electropromotion of methane combustion on palladium catalysts deposited on highly porous supports. *Appl. Catal. B Environ.* **2013**, *132–133*, 80–89. [CrossRef]

24. Jimenez-Borja, C.; Matei, F.; Dorado, F.; Valverde, J.L. Characterization of Pd catalyst-electrodes deposited on YSZ: Influence of the preparation technique and the presence of a ceria interlayer. *Appl. Surf. Sci.* **2012**, *261*, 671–678. [CrossRef]

25. Garbowski, E.; Feumi-Jantou, C.; Mouaddib, N.; Primet, M. Catalytic combustion of methane over palladium supported on alumina catalysts: Evidence for reconstruction of particles. *Appl. Catal. A Gen.* **1994**, *109*, 277–292. [CrossRef]

26. Vayenas, C.G.; Bebelis, S.; Yentekakis, I.V.; Lintz, H.-G. Non-faradaic electrochemical modification of catalytic activity: A status report. *Catal. Today* **1992**, *11*, 303–442. [CrossRef]

27. Nicole, J.; Comninellis, C.H. Electrochemical promotion of IrO_2 catalyst activity for the gas phase combustion of ethylene. *J. Appl. Electrochem.* **1998**, *28*, 223–226. [CrossRef]

28. Vayenas, C.; Brosda, S.; Pliangos, C. The double-layer approach to promotion, electrocatalysis, electrochemical promotion, and metal–support interactions. *J. Catal.* **2003**, *216*, 487–504. [CrossRef]

29. Reuter, K.; Scheffler, M. Composition, structure, and stability of RuO_2 (110) as a function of oxygen pressure. *Phys. Rev. B* **2001**, *65*, 035406. [CrossRef]

30. Gibson, I.R.; Dransfield, G.P.; Irvine, J.T.S. Sinterability of commercial 8 mol % yttria-stabilized zirconia powders and the effect of sintered density on the ionic conductivity. *J. Mater. Sci.* **1998**, *33*, 4297–4305. [CrossRef]

31. Hajar, Y.M.; Dole, H.A.; Couillard, M.; Baranova, E.A. Investigation of heterogeneous catalysts by electrochemical method: Ceria and titania supported iridium for ethylene oxidation. *ECS Trans.* **2016**, *72*, 161–172. [CrossRef]

32. Hajar, Y.M.; Patel, K.D.; Tariq, U.; Baranova, E.A. Functional equivalence of electrochemical promotion and metal support interaction for Pt and RuO$_2$ nanoparticles. *J. Catal.* **2017**, *352*, 42–51. [CrossRef]

33. Hajar, Y.M.; Houache, M.S.; Tariq, U.; Vernoux, P.; Baranova, E.A. Nanoscopic Ni interfaced with oxygen conductive supports: Link between electrochemical and catalytic studies. *Electrochem. Soc.* **2017**, *77*, 51–66. [CrossRef]